International Journal of Steel Structures (2022) 22(2):539–556
https://doi.org/10.1007/s13296-022-00589-z

Online ISSN 2093-6311
Print ISSN 1598-2351

Application of Machine Learning in Prediction of Shear Capacity of Headed Steel Studs in Steel–Concrete Composite Structures

Cigdem Avci-Karatas[1]

Received: 8 June 2021 / Accepted: 16 February 2022 / Published online: 10 March 2022

Abstract

Headed studs are generally utilized as shear connectors at the interface between steel and concrete in composite structures primarily to transfer longitudinal shear force. This paper presents regression methodologies to predict the shear capacity of headed steel studs by using the concepts of minimax probability machine regression (MPMR) and extreme machine learning (EML). MPMR is carried out based on a minimax probability machine classification. EML is an updated version of a single hidden layer feedforward network. From the experimental data presented in extensive literature, key input parameters influencing the shear capacity have been identified and consolidated. The identified parameters include (i) steel stud shank diameter, (ii) compressive strength of concrete, and (iii) tensile strength of headed steel stud. After careful examination of the data and their limits, about 70–75% of the mixed dataset comprising the range of the values has been used for developing MPMR and EML-based models. The input data has been normalized based on the limits of individual parameters. The remaining data has been utilized for verification of the developed models. It is observed that the predicted shear strength capacity is comparable with the experimental observations. Further, the efficacy of the models has been evaluated through several statistical parameters, namely; root mean square error, mean absolute error, the coefficient of efficiency, root mean square error to observation's standard deviation ratio, normalized mean bias error, performance index, and variance account factor. It is found that the R^2 value is 0.9913 and 0.9479, respectively, for the models developed based on the concepts of MPMR and EML, indicating that the predicted value is closer to the experimental data.

Keywords Headed stud · Steel–concrete composite structure · Shear strength · Minimax probability machine regression · Extreme machine learning · Statistical modeling technique

List of Symbols

a_i	Input weight vectors
A_s	Cross-sectional area of a headed stud
b_i	Bias values
C_{ca}	Actual shear force
$\overline{C}_{ca}$	Mean shear force
C_{cp}	Predicted shear force
d	Steel stud shank diameter
E_c	Young's modulus of concrete
E_s	Young's modulus of steel stud
f_c	Compressive strength of cubic
f'_c	Compressive strength of cylindrical concrete
f_u	Tensile strength of steel stud
g	Nonlinear activation function
h_s	Length of the stud shank
H	Hidden layer output matrix of neural network
L	Number of hidden layers
n	Number of steel studs
N	Number of datasets
P_u	Shear strength capacity
R^2	The coefficient of determination
s	Width of radial function
T	Transpose
var	Variance
x_i^a	Component of the input vector before normalization
x_i^n	Component of the input vector after normalization
x_i^{max}	The maximum value of all components of input vector before normalization
x_i^{min}	The minimum value of all components of input vector before normalization
y_i	Output values
α	Aspect ratio
β_i	Assigned weight vector

✉ Cigdem Avci-Karatas
cigdem.karatas@yalova.edu.tr

[1] Department of Transportation Engineering, Faculty of Engineering, Yalova University, 77200 Yalova, Turkey

β_0 Output of MPMR learning algorithm
γ Ratio of the minimum tensile strength to the yield stress of stud
γ_v Material safety factor
ϕ_{sc} Resistance safety factor

1 Introduction

It is a well-known fact that steel-composite structures are substantially more effective for studies on hazard and risk assessment strategies to mitigate seismic damage due to effective utilization of concrete in the compression and steel in the tension. It offers superior characteristics, such as high strength-to-weight ratio, enhanced flexural stiffness, faster and flexible construction, convenience for repair and retrofitting, and increased durability, compared to traditional reinforced concrete (RC) structures (He et al., 2010; Lin et al., 2014; Shanmugam & Lakshmi, 2001). In the steel–concrete composite system, shear connectors must achieve adequate strength and ductility. Shear connectors are in the form of angles, channels, headed studs, and perforated ribs, to name a few common forms. Shear connectors placed at the steel–concrete interface will transfer the stresses between both materials (Baran & Topkaya, 2012; Colajanni et al., 2014; Lam & El-Lobody, 2005).

To transfer longitudinal shear force at the interface of the steel–concrete composite system, the most commonly employed connectors are headed steel studs. The prime usage of the stud shear connectors can be seen in bridge decks. The performance of shear connector is related to several aspects, including (i) the geometry of headed stud, i.e., diameter, and height of the shank, (ii) stud tensile strength, (iii) concrete compressive strength and elastic modulus, (iv) weld quality of stud, and (v) the direction of concrete casting and reinforcement detailing. The shear strength of the headed stud is determined by performing either push-out or beam tests. Most of the recommended code provisions contain expressions to calculate the shear strength capacity of studs, which were obtained from experimental push-out tests. As summarized in Sect. 2 and Table 1, the capacity of studs depends on several aspects, namely, the use of studs in a type of composite structural element (such as composite slabs, walls, beams, push-out test specimens, etc.), the type of concrete (normal concrete, fiber RC, etc.), the embedment length of a stud in concrete, and failure mode. It can also be observed from Table 1 that comprehensive experiments considering the variation in (i) steel stud shank diameter, d, (ii) compressive strength of cylindrical concrete, f_c', and (iii) tensile strength of headed steel stud, f_u, to estimate the shear capacity are not available from a single source. Further, from Table 1, the key parameters were identified to develop and validate the models to predict the shear resistance of headed steel studs.

Various experiments were carried out to obtain the shear capacity of headed studs in the steel–concrete composite system under monotonic loading, cyclic loading, fatigue loading, and biaxial loading. In addition, the effects of various parameters, namely, concrete compressive strength, stud diameter, number of studs, and boundary conditions, on the shear strength, were investigated (Badie et al., 2002; Dogan & Roberts, 2012; Gattesco & Giuriani, 1996; Han et al., 2017; Kim et al., 2015; Shim et al., 2004; Valente & Cruz, 2009; Xu et al., 2015; Xue et al., 2008, 2012). Alternatively, the common failure phenomenon of studs in the steel–concrete composite system is the stud shank failure, embedment failure, splitting failure, and shear failure of a concrete slab (see Fig. 1) (Shim et al., 2004). Dennis (Dennis, 2007) proposed design equations to evaluate the shear connector's strength for headed steel stud connectors in precast hollow-core slabs. Besides, Nguyen and Kim (Nguyen & Kim, 2009) and Ellobody and Young (Ellobody & Young, 2006) developed a finite element model (FEM) considering nonlinearity to predict the composite behavior of headed stud shear connectors under push-out loading. Abambres and He (Abambres & He, 2019) adopted the artificial neural network (ANN) modeling approach to predict the shear resistance of headed steel studs by using the collected data from the literature. They found that the ANN-based model performs better compared to code-based equations [e.g., given by Eurocode 4 (EC4) (2004), AASHTO-LRFD (2014), and the Chinese Code GB50017 (2017)]. The expressions available in Codes of practice were determined to underestimate the shear capacity compared to experimental values (Abambres & He, 2019).

There are some regression or machine learning tools; namely, ANN, relevance vector machine (RVM), multivariate adaptive regression splines (MARS), support vector machine (SVM), Gaussian process regression (GPR), minimax probability machine regression (MPMR), extreme machine learning (also known as extreme learning machine) (EML), and least squares support vector machine (LS-SVM) available in the literature to develop models (Akbas et al., 2011; Al-Musawi, 2019; Avci-Karatas, 2019, 2021; Cao et al., 2020; DeRousseau et al., 2019; Dutta et al., 2018; Gholampour et al., 2020; Huang & Huang, 2020; Mansouri et al., 2017; Murthy et al., 2019; Shah et al., 2014) to predict the desired response. Comparatively, each model has its own merits and limitations. For instance, ANN provides benefits include not requiring an understanding of internal system parameters but rather a compact solution for multi-variable problems (Mansouri et al., 2019; Shariati et al., 2019). On the other hand, soft computing algorithm for single hidden layer feedforward neural network (NN) now is obtainable through EML (Huang et al., 2006a; Wang & Huang, 2005).

Table 1 Pervious investigations carried out on stud shear connections

Source	Investigations	
	Done/missing	Found/proposed
Viest (1956)	Stud shear connectors (*i.e.*, diameters ranging from 13*mm* to 32*mm*) were first tested under a static load in 12 push-out tests using varying depth-to-stud diameter ratios, (h_s/d), (equal to 2.47, 2.55, 3.23, 3.22, 4.53, 4.67, 4.77, 5.50, 7.00) to evaluate the shear strength of connectors. Three types of failure modes were observed, including (i) the stud connector fully yielded and no concrete failure, (ii) the concrete cone failure where no shearing off of headed stud, (iii) the combined failure of stud and concrete. The ranges of $f_c^{'}$ were between $22.0MPa - 30.2MPa$ for the type of normal concrete	Created an expression to calculate the shear strength of studs: $P_u = \begin{cases} 332d^2\sqrt{f_c'} & h_s/d \geq 4.2) \\ 79h_s d\sqrt{f_c'} & h_s/d \leq 4.2) \end{cases}$
Thurlimann (1959)	Studies with push-off were conducted using bent studs with a 13*mm* diameter and straight studs with a diameter of 19*mm* with a heads-up design	The concrete's strength and the diameter and height of the stud were found to be related to its shear capacity. The pull-off tests proved that steel studs could be used as shear connectors and that a stud connector would have similar behavior to a flexible channel connector
Driscoll and Slutter (1961)	Carried out flexural studies on steel–concrete composite beams to evaluate flexural strengths. Discussed the application of plastic design theory to composite beams. To demonstrate the validity of plastic theory, 13 composite beams and a wide variety of pushout specimens were tested. It was shown that shear tests embedded in normal-weight concrete would have sufficient shear capacity, provided that their height was increased	According to the AISC specifications, which are based on the findings of Driscoll and Slutter (Driscoll & Slutter, 1961), the center-to-center spacing of stud connectors shall be limited to 6*d* along the longitudinal axis of the supporting beam and to 4*d* transverse to that axis. It was determined that studs fail not in shear, but in tension, and their ultimate strength is based on tensile strength. Researchers penalized studies with a height to diameter ratio (h_s/d) less than 4.2 because of the possibility of reduced concrete strength. Determined the shear strength of studs for the composite structure using the following expression: $P_u = 222h_s d\sqrt{f_c'}/A_s$
Slutter and Driscoll (1965)	Carried out a test program included 36 beam tests as well as push-out specimens of 21 headed studs, 10 spiral connectors, and 41 channel connectors. Analyzed the relationship between shear connector strength and concrete compressive strength. This methodology was compared with Viest's (1956) shear bearing capacity formula. Earlier researchers were very concerned about how slip affects the completeness of interactions between the slab and beam. When considering the ultimate strength of members, this factor was ignored in this study. Shown that slip is not an important parameter when considering the ultimate strength of members if the number of shear connectors is adequate	In the AISC Specifications, the allowable loads for stud shear connectors embedded in normal-weight concrete are based on the model suggested by Slutter and Driscoll (Slutter & Driscoll, 1965). Found that previous investigators had ignored the ultimate strength of connectors, and with their study, some reliable data on this property was produced. Proposed a formula for calculating the shear bearing capacity of studs when their concrete strength is no more than 28*MPa*: $P_u = \begin{cases} 220h_s d\sqrt{f_c'} & h_s/d \leq 4.1) \\ 930d^2\sqrt{f_c'} & h_s/d \geq 4.1) \end{cases}$
Ollgaard et al. (1971)	Developed a model to measure the strength of shear studs in lightweight concrete (30 tests) and normal-weight concrete (18 tests) that became the basis for the development of codes for solid reinforced concrete slabs. During this investigation, 48 two-slab pushout specimens were tested. There were two types of normal-weight aggregates and three types of lightweight aggregates studied. The effective depth-to-stud diameter ratios were 3.50 and 4.41, and the ranges of $f_c^{'}$ were from 18.4*MPa* to 35.0*MPa*	Proposed the first formula for calculating the shear strength of headed studs that was adopted by the AISC Manual in 1993: $P_u = 0.5A_s\sqrt{E_c f_c'}$

Table 1 (continued)

Source	Investigations	
	Done/missing	Found/proposed
Menzies (1971)	Studied steel–concrete composite beams with shear connectors in which the concrete consists of normal-density concrete and lightweight concrete. A comparison of that code's shear connector strength and the results of his push-off tests was conducted. Experimentally examined the effect of concrete strength and density on the static and fatigue strength of connectors using 34 push-off test specimens. The effective depth-to-stud diameter ratio was 4.67, and the ranges of $f_c^{'}$ were between $17.0MPa - 50.5MPa$	Found that the specified shear connector strength listed in CP 117 should be modified in order to encompass a broader range of concrete strengths; a distinction should be made between connectors embedded in normal-density concrete and lightweight concrete. The study concluded that CP 117 overestimated stud strength in lightweight concrete when the density is below $1400kg/m^3$
Hawkins (1973)	Tested 47 push-out specimens for stud shear connectors in composite steel and concrete construction. Tests were conducted on specimens with studs of various dimensions and slabs with and without reinforcement were also tested. The effective depth-to-stud diameter ratios were $2.00, 2.33, 2.86, 3.00, 3.51, 4.00, 4.67$, and the ranges of $f_c^{'}$ were between $19.9MPa - 34.7MPa$. Comparisons are made between the test results and those of other investigators, as well as those of the AISC specification and British code CP 117	Found that by modeling the connector as a flexible elastic dowel on an elastic foundation, the curves of stress slip for low loads could be predicted. A theoretical expression was developed to explain the relative influences of the variables examined on high loads
Oehlers and Johnson (1987)	Evaluated the shear capacity of studs in composite beams. Calculated the static strength of stud shear connections in composite beams using 110 push tests, including eight tests that measured axial loads applied to the connectors. The effect of individual connectors on longitudinal shear flow in steel–concrete composite beams over steel flanges/concrete slabs was investigated	Shear connections are found to have a strength less than 20% of their theoretical strength when cracks split. It was determined that the transverse reinforcement limited the strength of the split and allowed a gradual reduction of the shear load after splitting. Developed a formula that includes contributions from both studs and concrete. Determined the mean strength of stud connectors by: $P_u = KA_s\left(\frac{E_c}{E_s}\right)^{0.4}\left(\frac{f_c}{f_u}\right)^{0.35}$ where $K = 4.1 - n^{-1/2}$
Hiragi et al. (2003)	Researchers set out to reevaluate the testing methods and existing proposals of pull-out and shear strength of the stud, as well as to collect and reorganize both the domestic and foreign tested data, including the results obtained by the authors. There are several factors that influence the strength of a stud, and the estimating equations for pull-out and shear strength are discussed both with and without considering edge distances. There were 294 basic statistical data for pull-out strength in testing, 197 for push-out shear strength in tests for double shear surfaces, and 118 for push-out shear strength in single shear tests	The design strength formulas which take the scattering of tested data into account were revised by a reduction factor, (α_q): $P_u = 31A_s\sqrt{(\frac{h_s}{d})f_c^{'}} + \alpha_q$
Shim et al. (2004)	18 push-out tests were conducted on large stud shear connectors with diameters of $25mm, 27mm, 30mm$, and compared with EC4. There were effective depth-to-stud diameter ratios of $5.68, 5.22, 4.70$, and the ranges of $f_c^{'}$ were $35.3MPa - 64.4MPa$	A trilinear load slip curve was proposed by testing studs for shear stiffness and trilinear shear stiffness in an elastic range

Table 1 (continued)

Source	Investigations	
	Done/missing	Found/proposed
Zhou et al. (2008)	Evaluated the shear capacity and shear rigidity of stud connectors. Pull-off tests were conducted on stud shear connectors under tension with a concrete slab. Bearing capacity was determined from the Chinese standard for the 12 studs with diameters of $16mm, 19mm, 22mm$. The concrete cube strengths, f_c, were $50.9MPa, 41.0MPa$, and $31.5MPa$	Determined that the stud diameter has a noticeable influence on ultimate carrying capacity, while concrete intensity and steel fibers do not have a significant influence on ultimate carrying capacity. Findings revealed that the longitudinal steel bar does not yield before the stud is failed with a shear connection degree less than 1.0; the bearing capacity of the stud does not differ significantly with concrete under tension and compression. It was suggested to decrease the bearing capacity in the current specification by 10%
Xue et al. (2008)	Analyzed the mechanism of shear based on the experimental results. A total of 30 push-out tests on studs was carried out and the effects of stud diameter and height (*e.g.*, $13mm$, $16mm$, and $19mm$), concrete strength, stud welding technique, transverse reinforcement, and beam type were investigated and compared with existing models	An expression accounting for the effect of stud diameter and height, material strength, and elastic modulus was proposed to estimate the shear capacity: $P_u = 3\lambda A_s f_u \left(\frac{E_c}{E_s}\right)^{0.4} \left(\frac{f_c}{f_u}\right)^{0.2}$ where $\lambda = \begin{cases} 6 - \frac{H}{1.05d}\left(\frac{h_s}{d} \le 5\right) \\ 1\left(5 < \frac{h_s}{d} < 7\right) \\ \frac{h_s}{d} - 6\left(\frac{h_s}{d} \ge 7\right) \end{cases}$
Pallarés and Hajjar (2010)	A literature review of 391 monotonic and cyclic tests of headed stud anchors was performed along with tests on headed steel stud anchors in steel–concrete composite structures	Provided recommendations for the seismic behavior of headed studs based on shear strength values. In the context of the 2005 AISC Specification, formulas were proposed to determine the limit states of steel failure and concrete failure of headed stud anchors subjected to shear force without using a metal deck, and comparisons were made to provisions in the ACI 318–08 Building Code, PCI Handbook, 6th Edition, and EC 4
Xue et al. (2012)	Investigated the behavior of single and multi-stud connectors, and found that the maximum strength of single stud connector is higher (approximately 10%) compared to multi-stud connectors	Proposed a new expression of stud load-slip relationship based on the results of ten push-out tests. Shown that estimations based on EC4 agree well with multi-study test results, and estimations based on AASHTO-LRFD and Chinese code GB50017 agree well with single-study test results
Wang (2013)	Evaluated the mechanical behavior of stud connectors	Proposed a design method for stud connectors

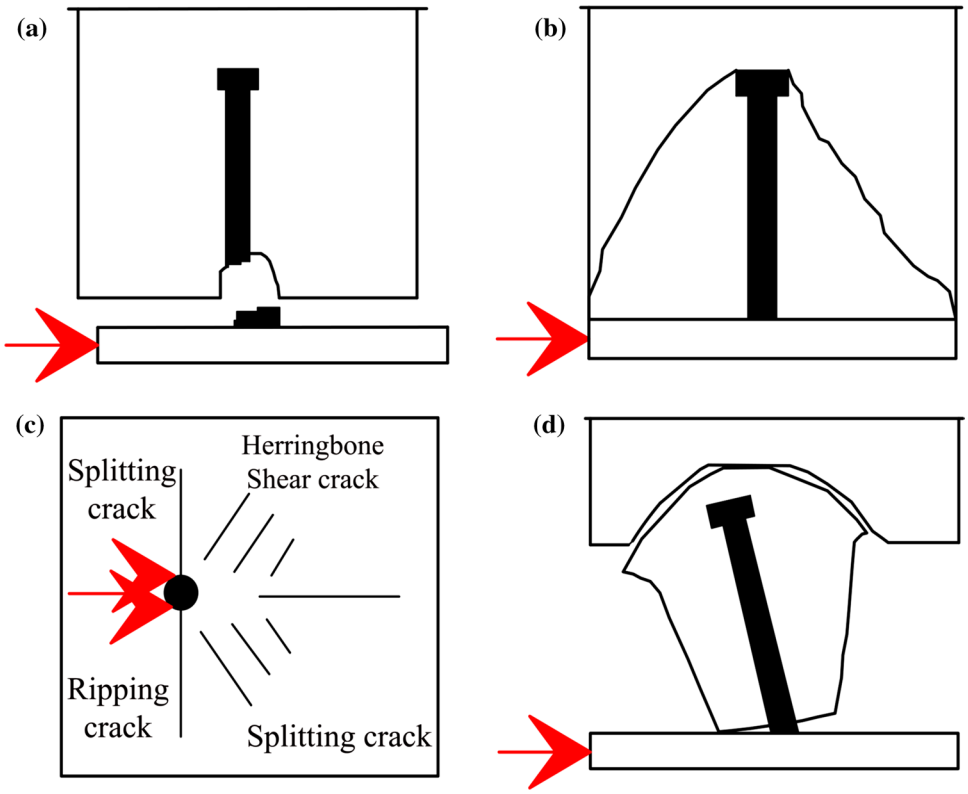

Fig. 1 Failure modes: **a** shank failure; **b** embedment failure; **c** slab cracking; **d** shear failure of slab (Figure adopted from Shim et al., 2004)

In comparison with ANN, EML-based model decreases the required time to train NN and could solve the problems caused by backpropagation, a gradient descent-based algorithm applied in ANNs. A reliable and accurate alternative analytical model considering these issues as compatible with real conditions of the shear resistance of headed steel studs has motivated the research and was analytically investigated in this paper. With the motivation on "quick learning" and "better performance" (Cao et al., 2020), the main objective of this investigation is the use of MPMR and EML-based modeling approaches.

Therefore, this study aims to develop a model to estimate the shear resistance of headed steel studs by applying the concepts of MPMR and EML. The novelty of this research is the utilization of comprehensive data to predict shear strengths of headed steel studs through machine regression tools. Generally speaking, it can be noted that applying both concepts in civil/structural engineering is found to be limited in the literature. Thus far, to the knowledge of the author, while steel–concrete composite structures have merit in seismic applications, and also, several analytical models were reported on evaluating the shear strength of headed steel studs in steel–concrete composite structures, no guidance exists to help the engineers for predicting shear capacities using EML and MPMR with a reasonable degree of accuracy in the current technical literature. In this study, the experimental behaviors of various headed steel studs, obtained from the push-out tests on shear connector behavior in steel–concrete joints, are consolidated and developed an analytical models by using the concepts of EML and MPMR to predict the shear strength capacity of headed steel studs. The models have been developed and verified with a dataset covering 234 experimental data results available in the literature. Based on the results given in Dutta et al. (Dutta et al., 2018), Murthy et al. (Murthy et al., 2019), DeRousseau et al. (DeRousseau et al., 2019), and Huang and Huang (Huang & Huang, 2020), the portions of the dataset has been decided to develop and validate the model. After referring to the mentioned literature related to the developed regression models, 70–75% of the dataset has been decided to develop the models and the rest of the data has been used for validation. It is noteworthy to mention in the present research that the developed MPMR and ELM-based modeling approaches will serve as reliable tools to predict the shear resistance of headed steel studs and will have a broader impact on the civil engineering profession. The findings of the paper are new and will make significant contributions to the existing technology of stud shear connectors in composite constructions.

The basic ideology of MPMR is to maximize the minimum probability of future data points during the classification process. Hence, the most featured aspect of MPMR is that it will provide exclusively a lower bound on the

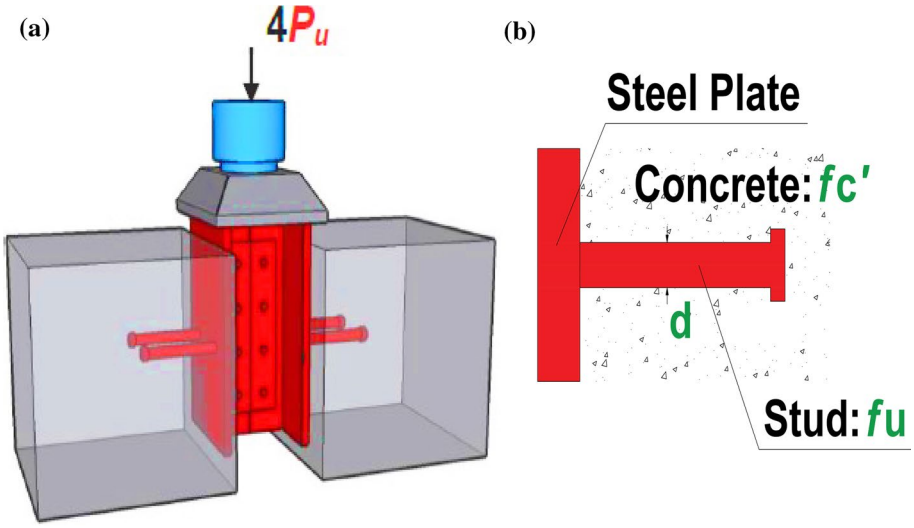

Fig. 2 Input (marked in green color) and target (marked in red color) parameters: **a** push-out test specimen; **b** headed steel stud (Figure adopted from Abambres & He, 2019)

probability that the model is within a defined error of the true regression function when the mean and covariance/auto-covariance matrix of the data are known. EML is an improved version of a single hidden layer feedforward neural network (SLFN). Shah et al. (2014) and Parab et al. (2014) predicted fracture parameters of high strength and ultra-high-strength concrete beams using GPR, LS-SVM, MPMR, and EML. An analytical prediction model using the concepts of MPMR and GPR for hardness and fracture toughness of liquid-phase-sintered alumina system was proposed by Gopinath et al. (2018). In an attempt to provide quantitative data for predicting the shear resistance of headed studs in steel–concrete composite structures through MPMR and EML, after providing a relevant literature review in this section, the remainder of the paper is arranged as follows: Sect. 2 illustrates the experimental data collection on the shear capacity of headed steel studs; Sect. 3, and Sect. 4 present the structure and implementation of the performed nonlinear machine learning algorithms giving a brief theory on MPMR and EML; Sect. 5 includes the development of MPMR and EML-based models for predicting the shear resistance of headed steel studs and validation check studies; and a comparison of MPMR and EML-Based Models with existing calculation methods is given in Sect. 6. Finally, Sect. 7 summarizes the major findings and perceived limitations of the current study.

2 Data Collection

Many other parameters definitely influence the stud capacity, such as the type of composite structural elements (e.g., composite slabs, walls, beams, push-out test specimens, etc.), the geometrical properties (e.g., head to shank diameter ratio, embedment length of the stud in concrete, head to shank length ratio, etc.), the concrete material types (e.g., normal concrete, high-performance concrete with strain hardening capacity, fiber RC, etc.), and failure modes. Figure 1 presents the common failure phenomenon of a stud in the steel–concrete composite system (Shim et al., 2004). In this research, data has been collected from the push-out tests on shear connector behavior in steel–concrete joints. Figure 2a shows a typical test setup, where a steel profile is attached to concrete slabs through the shear connectors. About 234-point dataset has been collected from various sources (Driscoll & Slutter, 1961; Hawkins, 1973; Hiragi et al., 2003; Menzies, 1971; Oehlers & Johnson, 1987; Ollgaard et al., 1971; Pallarés & Hajjar, 2010; Shim et al., 2004; Slutter & Driscoll, 1965; Thurlimann, 1959; Viest, 1956; Wang, 2013; Xue et al., 2008, 2012; Zhou et al., 2008) [Developer 2018a available in Reference (Abambres & He, 2019)]. Table 1 briefly presents experimental details, such as geometrical parameters, material properties of input, and target/output variables that were conducted by several researchers mentioned above. From these experimental studies, it was observed that the shear strength of steel stud, P_u, primarily related to three parameters; namely, (i) steel stud shank diameter, d, (ii) 28-day compressive strength of cylindrical concrete, $f_c^{'}$, and (iii) tensile strength of headed steel stud, f_u. These parameters have been considered central input variables for the developing models. Figure 2b clarifies the input and the expected output parameters proposed for developing the models. Table 2 presents the consolidated experimental data.

To ease the implementation of predictive model by any interested researchers while alleviating the issues related to the practical applications of the models, only three variables,d,$f_c^{'}$, andf_u, are assumed in this study to determine the shear capacity of studs since those were the key parameters affect the shear failure of headed steel studs. It was noticed that the effect of other parameters, such as the connector

Table 2 Experimental data on shear strength capacity of headed steel studs, P_u^E, in the steel–concrete composite system

Input				Output	Input				Output
Data point	d (mm)	$f_c^{'}$ (MPa)	f_u (MPa)	P_u^E (kN)	Data point	d (mm)	$f_c^{'}$ (MPa)	f_u (MPa)	P_u^E (kN)
1	19.50	38.00	388.50	122.90	50	19.00	31.50	468.00	134.00
2	19.00	55.70	415.00	117.00	51	27.00	62.70	400.00	228.00
3	25.00	35.80	485.00	235.50	52	16.00	55.70	326.00	67.80
4	13.00	60.00	425.00	59.40	53	30.00	36.80	366.00	253.40
5	15.90	33.90	483.70	93.10	54	30.00	36.80	477.00	333.80
6	12.70	51.10	439.80	57.90	55	19.50	32.40	482.10	138.30
7	25.00	40.10	380.00	184.30	56	27.00	68.80	420.00	233.70
8	13.00	70.00	425.00	60.60	57	22.00	70.30	465.00	180.40
9	22.00	45.60	478.00	179.40	58	22.00	40.00	375.00	138.40
10	19.00	50.50	495.00	142.10	59	22.00	45.60	380.00	140.20
11	22.00	70.00	417.00	163.10	60	22.00	55.70	514.00	199.00
12	19.00	50.00	495.00	141.30	61	19.00	30.00	495.00	118.70
13	22.00	35.00	470.00	175.10	62	19.00	32.20	455.00	130.60
14	19.50	37.40	421.30	128.80	63	19.00	27.60	460.00	110.90
15	25.00	56.30	515.00	253.60	64	16.00	56.50	455.00	92.60
16	19.50	30.10	488.50	129.90	65	19.00	22.80	420.00	98.80
17	19.50	45.00	488.50	147.10	66	30.00	66.20	460.00	331.00
18	22.00	59.90	430.00	158.00	67	19.50	45.90	466.80	138.80
19	15.90	31.20	327.00	67.00	68	30.00	70.30	478.00	342.00
20	10.00	25.50	335.00	26.20	69	19.00	100.10	519.00	153.80
21	19.50	37.80	305.70	90.50	70	22.00	28.00	355.00	129.30
22	30.00	59.30	535.00	381.00	71	16.00	30.00	335.00	70.20
23	22.00	54.60	445.00	174.90	72	13.00	66.30	445.00	60.30
24	16.00	40.00	455.00	88.90	73	10.00	39.20	465.00	38.50
25	22.00	40.00	417.00	154.40	74	19.00	40.30	519.00	147.10
26	9.50	39.30	435.00	28.60	75	25.00	48.80	455.00	220.80
27	19.00	54.60	445.00	135.50	76	27.00	62.70	460.00	270.20
28	22.00	60.00	417.00	161.00	77	27.00	35.60	375.00	214.90
29	22.00	28.00	417.00	151.90	78	30.00	43.50	455.00	317.00
30	19.00	20.50	495.00	93.80	79	19.00	58.50	425.00	123.00
31	12.70	47.80	457.60	60.90	80	15.90	31.60	469.00	90.90
32	22.00	30.00	450.00	162.60	81	19.00	55.70	425.00	121.00
33	22.00	28.00	378.00	141.20	82	22.00	50.50	515.00	197.20
34	19.00	20.00	470.00	92.00	83	16.00	50.50	455.00	92.10
35	19.50	33.00	397.40	123.30	84	19.00	30.80	460.00	127.90
36	12.70	36.70	452.80	58.40	85	27.00	50.50	390.00	224.30
37	19.00	55.70	435.00	124.00	86	22.00	31.50	468.00	176.30
38	16.00	39.10	462.00	93.00	87	19.00	38.40	455.00	134.20
39	19.00	70.00	495.00	147.00	88	25.00	35.80	380.00	181.60
40	25.00	40.10	430.00	210.20	89	25.00	54.10	455.00	224.50
41	30.00	36.80	424.00	290.70	90	22.00	54.10	534.00	204.00
42	13.00	50.00	455.00	60.50	91	27.00	45.70	385.00	222.00
43	22.00	25.20	415.00	143.70	92	19.00	50.00	420.00	114.95
44	25.00	50.00	500.00	246.10	93	15.90	35.50	419.30	84.40
45	22.00	40.00	468.00	178.50	94	22.00	55.70	500.00	189.00
46	30.00	52.60	478.00	341.00	95	13.00	40.00	425.00	56.00
47	15.90	36.00	436.60	88.00	96	19.50	45.90	404.90	126.60
48	25.00	50.00	420.00	211.60	97	22.00	35.00	435.00	159.80
49	27.00	68.80	520.00	294.80	98	22.00	55.70	530.00	201.00

Table 2 (continued)

Input				Output	Input				Output
Data point	d (mm)	$f_c^{'}$ (MPa)	f_u (MPa)	P_u^E (kN)	Data point	d (mm)	$f_c^{'}$ (MPa)	f_u (MPa)	P_u^E (kN)
99	30.00	66.20	525.00	368.00	148	27.00	56.00	458.00	268.20
100	22.00	45.60	435.00	162.50	149	25.00	54.10	495.00	248.10
101	12.70	48.60	412.50	56.70	150	9.50	47.60	435.00	30.40
102	30.00	52.60	420.00	290.00	151	27.00	41.10	490.00	284.40
103	22.00	25.00	345.00	128.60	152	15.90	42.10	472.00	92.60
104	30.00	43.50	389.00	278.00	153	25.00	44.60	445.00	216.50
105	27.00	30.50	430.00	242.80	154	25.00	40.10	485.00	236.40
106	15.90	35.50	321.50	68.10	155	19.00	109.30	519.00	156.00
107	30.00	59.30	488.00	340.00	156	16.00	30.00	455.00	87.40
108	19.50	37.80	385.10	121.90	157	13.00	49.80	450.00	60.10
109	15.90	42.10	436.40	90.00	158	12.70	51.00	443.20	58.60
110	27.00	30.50	479.00	253.10	159	13.00	30.00	425.00	54.10
111	19.50	28.20	466.90	123.30	160	16.00	30.00	420.00	82.45
112	25.00	44.60	490.00	242.20	161	25.00	50.00	455.00	222.00
113	19.00	55.00	495.00	145.00	162	19.50	23.00	488.50	101.50
114	27.00	62.70	515.00	292.20	163	15.90	31.20	470.60	87.00
115	19.00	38.10	519.00	145.00	164	16.00	70.00	455.00	94.10
116	12.70	38.00	450.10	59.10	165	13.00	50.10	425.00	57.10
117	27.00	30.50	380.00	213.40	166	16.00	24.50	335.00	66.20
118	22.00	50.00	510.00	190.70	167	30.00	70.30	595.00	415.00
119	15.90	36.90	406.30	82.20	168	25.00	44.60	390.00	188.90
120	22.00	50.00	477.00	181.00	169	13.00	39.20	469.00	60.40
121	16.00	41.00	468.00	93.80	170	25.00	48.80	495.00	244.10
122	16.00	60.00	455.00	93.20	171	19.50	27.50	477.90	121.10
123	27.00	35.60	435.00	246.80	172	16.00	55.90	326.00	68.10
124	27.00	35.60	485.00	272.90	173	19.00	44.00	450.00	136.20
125	22.00	35.00	370.00	136.20	174	16.00	25.50	335.00	67.80
126	19.00	60.00	485.00	140.00	175	19.00	41.00	468.00	136.00
127	19.00	50.50	515.00	144.20	176	13.00	34.50	435.00	56.80
128	27.00	45.70	495.00	287.50	177	15.90	35.50	484.30	97.90
129	19.50	37.40	426.10	130.20	178	19.50	38.00	409.70	125.60
130	12.70	32.10	487.60	62.10	179	25.00	70.30	535.00	265.60
131	25.00	48.80	375.00	187.50	180	19.00	50.50	535.00	151.00
132	19.00	20.00	495.00	93.10	181	25.00	54.10	534.00	263.00
133	19.00	39.50	495.00	139.10	182	22.00	55.70	475.00	186.80
134	22.00	30.00	425.00	155.50	183	12.70	48.60	463.10	60.70
135	27.00	56.00	392.00	226.40	184	19.00	55.70	475.00	139.00
136	19.00	50.00	470.00	137.00	185	27.00	41.10	445.00	250.10
137	19.00	55.00	477.00	141.00	186	15.90	35.50	437.80	88.20
138	22.00	63.40	519.00	202.20	187	19.50	45.90	495.60	145.10
139	22.00	30.00	365.00	133.60	188	12.70	38.00	452.80	59.80
140	19.00	39.10	462.00	135.00	189	27.00	45.70	455.00	264.20
141	16.00	55.10	326.00	67.00	190	19.00	30.00	420.00	111.50
142	27.00	56.00	497.00	290.90	191	9.50	32.40	435.00	27.90
143	30.00	66.20	575.00	410.00	192	19.50	38.00	434.30	131.20
144	19.00	95.90	519.00	151.90	193	27.00	41.10	378.00	217.90
145	30.00	70.30	545.00	388.00	194	25.00	35.80	430.00	208.70
146	19.00	33.00	460.00	133.10	195	15.90	31.20	420.00	80.80

Table 2 (continued)

Input				Output	Input				Output
Data point	d (mm)	$f_c^{'}$ (MPa)	f_u (MPa)	P_u^E (kN)	Data point	d (mm)	$f_c^{'}$ (MPa)	f_u (MPa)	P_u^E (kN)
147	22.00	31.50	430.00	157.50	196	19.50	35.90	485.50	144.60
197	19.00	38.70	519.00	146.80	216	19.00	30.60	460.00	125.70
198	19.00	27.00	460.00	108.80	217	25.00	57.30	426.00	213.70
199	27.00	68.80	465.00	271.80	218	13.00	25.00	335.00	43.00
200	12.70	51.10	459.60	60.50	219	19.00	50.90	468.00	138.10
201	22.00	31.50	350.00	134.00	220	27.00	50.50	460.00	267.80
202	19.50	41.70	488.50	146.00	221	22.00	60.00	450.00	176.00
203	22.00	28.80	420.00	153.40	222	22.00	50.00	455.00	173.70
204	27.00	50.50	500.00	289.60	223	15.90	33.70	483.70	91.50
205	19.00	18.30	420.00	85.80	224	22.00	60.10	500.00	190.60
206	22.00	50.90	470.00	183.00	225	12.70	38.00	449.40	58.90
207	22.00	50.00	420.00	160.70	226	12.70	36.70	446.00	58.70
208	30.00	52.60	521.00	372.00	227	19.00	19.80	420.00	90.30
209	9.50	36.60	435.00	28.20	228	12.70	48.60	523.90	64.90
210	22.00	25.20	375.00	139.50	229	16.00	50.00	420.00	88.40
211	19.50	33.00	417.90	127.40	230	19.50	37.80	342.00	102.00
212	9.50	45.50	435.00	29.10	231	12.70	36.70	451.40	57.80
213	12.70	48.60	465.10	61.40	232	12.70	37.40	488.30	61.80
214	19.00	40.00	495.00	140.20	233	30.00	59.30	438.00	313.00
215	30.00	43.50	513.00	358.00	234	19.50	37.40	378.30	120.20

length, and arrangement (spacing, pattern), the weld quality, weld dimensions, the friction properties, and orientation of the steel–concrete interface during concreting, is minimum on the shear capacity (Chen et al., 2019; Driscoll & Slutter, 1961; Ellobody, 2014; Hawkins, 1973; Hiragi et al., 2003; Menzies, 1971; Oehlers & Johnson, 1987; Ollgaard et al., 1971; Pallarés & Hajjar, 2010; Shim et al., 2004; Slutter & Driscoll, 1965; Thurlimann, 1959; Viest, 1956; Wang, 2013; Xue et al., 2008, 2012; Zhou et al., 2008). For example, the shear capacity is slightly influenced by stud length when the length-to-diameter ratio (h_s/d) is larger than 4 (Abambres & He, 2019; ANSI & AISC, 2016; ANSI & AISC-360-16, 2016; Chen et al., 2019; Driscoll & Slutter, 1961; Ellobody, 2014). The experimental data here about the stud specimens having the length-to-diameter ratio are more than4. To validate the models considering more variables may not easily be applied for every structural, geometrical, and material type since each has its own merits. The aim of the developed models in the present investigation is to provide a unique study to the researcher to obtain the decreasing errors, complexity, and reducing convergence of scattering amplitudes of numerical results to experimental ones that can be an alternative to additional experimental studies. The minimum, maximum, and average values of input variable d are 9.5mm, 30mm and 20.4mm, for $f_c^{'}$, the values are18.3MPa, 109.3MPa and 44.6MPa, and for f_u, the values are 305.7MPa, 595MPa, and 448.4MPa, respectively. These variations

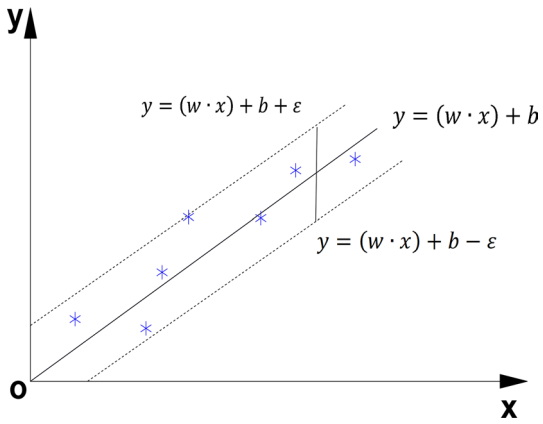

Fig. 3 Typical MPMR algorithm

have been considered while producing model processes to increase the possibility of obtaining a more robust model.

3 Minimax probability machine regression (MPMR)

MPMR, an alternative justification for discriminative techniques, is considered in several applications in the literature (Sun, 2009; Yang et al., 2010; Zhou et al., 2013). The basic

mission of MPMR is to maximize the minimum probability of future data points during the classification process. The benefit of the MPMR model includes the minimum assumption of underlying distribution for true function in trivial regression problems within their bounds. This focus of MPMR is based on the minimax probability machine classification (MPMC) algorithm proposed by Lanckriet et al. (2001), which employs Mercer's kernel functions to obtain nonlinear regression models with nonlinear classifiers (i.e., MPMC) that maximize the minimum probability of correct classification on future data. For the case of nonlinear models, the general basis function is given by Eq. (1).

$$f(x) = \sum_{i=1}^{m} \beta_i \varphi_i(x) + \beta_0 \tag{1}$$

where, β_i and β_0 are outputs, $\varphi_i(x)$ is the kernel function. As in the support vector machine, the kernelized version of the MPM can also be constructed by mapping the input vectors into a high-dimensional feature space F, where the linear regression in F corresponds to a nonlinear regression in the original input spaces. Based on the mapping function, Eq. (1) can be expressed as follows:

$$\hat{y} = \hat{f}(x) = \sum_{i=1}^{N} \beta_i K\left(x_i, x\right) + b \tag{2}$$

where, $K\left(x_i, x\right) = \varphi(x_i)\varphi(x)$ is a kernel satisfying Mercer's conditions, $x_i, \forall_i \in \{1, \ldots, N\}$ is obtained from the input/learning data, Γ', and $\beta_i, b \epsilon \Re$ are the outputs of the MPMR learning algorithm (Strohmann & Grudic, 2002).

In the present problem, 'x' is the function of steel stud shank diameter (d), the compressive strength of concrete (f_c'), the tensile strength of stud (f_u), and the output of MPMR is stud shear force at failure (P_u), which are also represented as $x = \left[(d), \left(f_c'\right), \left(f_u\right)\right]$ and $y = [P_u]$ for the prediction of shear force. MPMR has been developed by constructing a dichotomy classifier. As mentioned earlier, it is proposed to develop MPMR methodologies in the framework of MPMC to build a classifier that separates two sets of points. Figure 3 pictorially represents the typical MPMR algorithm, in which the classification boundary is located between the regression data $+\varepsilon$ and $-\varepsilon$. As the datasets (input and output) have different quantitative limits, they are to be normalized before use in the model development. The effect of the radial function is significant on the performance of the model. In the present study, the radial basis function (RBF) is expressed as follows:

$$K\left(x_i, x\right) = exp\left[-\frac{(x_i - x)(x_i - x)^T}{2s^2}\right] \tag{3}$$

where s is the width of radial basis function, and T is the transpose as covariance function.

4 Extreme Machine Learning (EML)

In feedforward neural networks (FNNs), gradient descent-based methods (methods of steepest descent) are commonly used. However, the performance of these methods is not efficient due to improper learning steps, and it requires more iterations to achieve better performance. EMLs are based on FNNs with single or multiple hidden layers. Conventionally, the various entities of feedforward networks are to be modified or tuned for better performance. The principal advantage of EML is no need to change or edit the entities of hidden nodes while producing the model. Meanwhile, the hidden nodes can be randomly assigned based on experience and judgment. Huang and Babri (1998) proposed a new machine learning algorithm, called single hidden layer feedforward neural networks (SLFNNs), whose efficiency is much faster compared to the ANN model. This new algorithm is called EML. EML randomly chooses hidden nodes and rationally decides the output weight of SLFNNs. The formulation adopted in the present study is the modified version of SLFNN proposed by Huang et al. (2006b). The relation varying between input (x) and output (y) is calculated from Eq. (4).

$$\sum_{i=1}^{L} \beta_i g_i\left(x_j\right) = \sum_{i=1}^{L} \beta_i G\left(a_i, b_i, x_j\right) = y_j, j = 1, \ldots, L \tag{4}$$

where, L is the number of hidden layers, g is the nonlinear activation function, β_i is the assigned weight vector, a_i is the input weight vectors, b_i is bias values or threshold value for $i = 1, \ldots L$, and y_j is the output value. Equation (4) can be modified as:

$$H\beta = T \tag{5}$$

H is known as the hidden layer output matrix of the neural network; the i th column of H is the i th hidden neuron's output vector for input $x_1, x_2, \ldots, x_N$. H, β, and T are stated by Eqs. (6), (7), and (8) as follows:

$$H = \begin{bmatrix} G(a_1, b_1, x_1) & \cdots & G(a_L, b_L, x_1) \\ \vdots & \ddots & \vdots \\ G(a_1, b_1, x_N) & \cdots & G(a_L, b_L, x_N) \end{bmatrix}_{N \times L} \tag{6}$$

$$\beta = \begin{bmatrix} \beta_1^T \\ \vdots \\ \beta_L^T \end{bmatrix}_{L \times m} \tag{7}$$

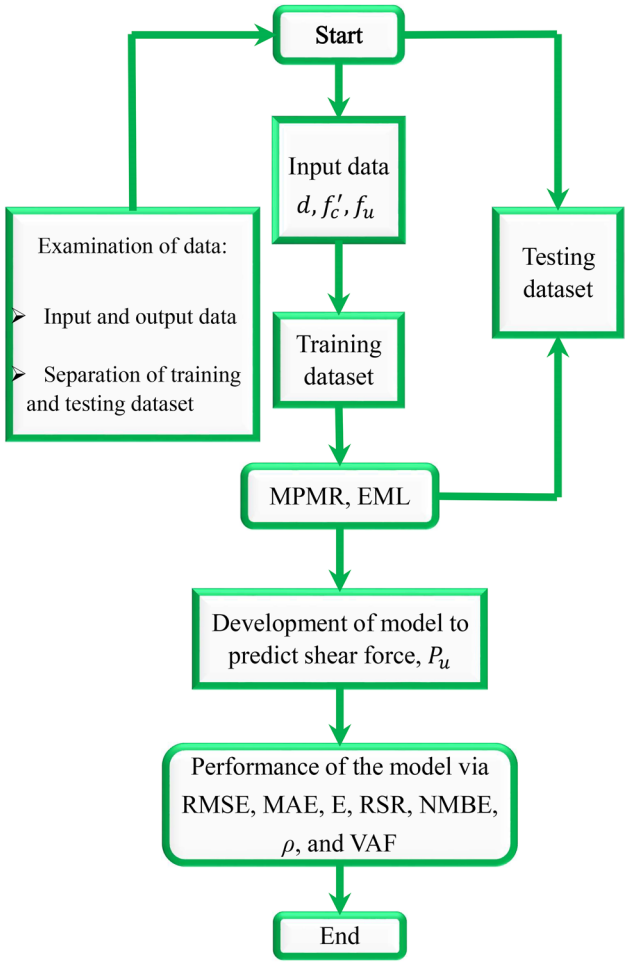

Fig. 4 Typical flowchart for the development of MPMR and EML models

$$T = \begin{bmatrix} y_1^T \\ \vdots \\ y_N^T \end{bmatrix}_{N \times m} \tag{8}$$

The output weight matrix, β, is computed through Eq. (9) as follows:

$$\beta = H^{-1}T \tag{9}$$

where, H^{-1} is Moore–Penrose generalized inverse (pseudo-inverse) of H. The input data, output data, normalization process, and radial basis function will be the same for both models. The algorithm to the analysis of data for EML based model with a four-step can shortly be summarized as below:

Step 1: a_i and b_i are assigned randomly.

Step 2: H is reckoned by using Eqs. (6), (7), and (8)

Step 3: β is reckoned by using Eq. (9)

Step 4: The output can be approximated by using Eq. (5)

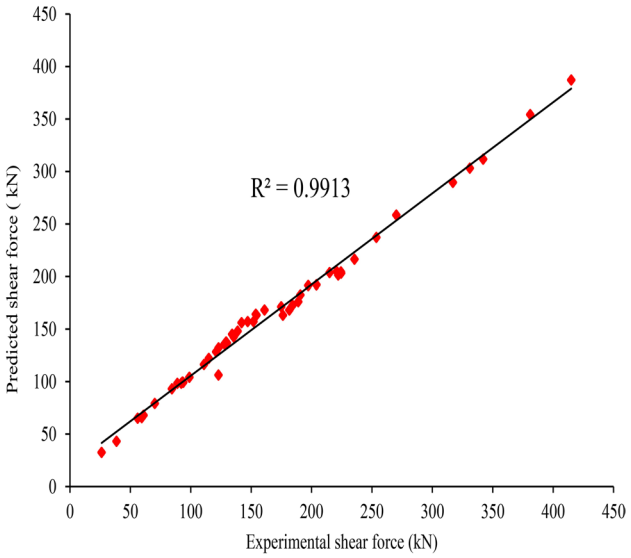

Fig. 5 Predicted and experimental shear forces for the proposed MPMR model

5 Development of MPMR and EML Based Models and Validation

This comprehensive paper presents an alternative numerical study to develop models based on the concept of MPMR and EML using MATLAB® R2016a environment with appropriate modifications. As can be observed in Table 2, P_u is primarily dependent on the parameters of d, $f_c^{'}$, and f_u, respectively. Further, it can be observed that these parameters cover sufficiently wide practical different limits, such

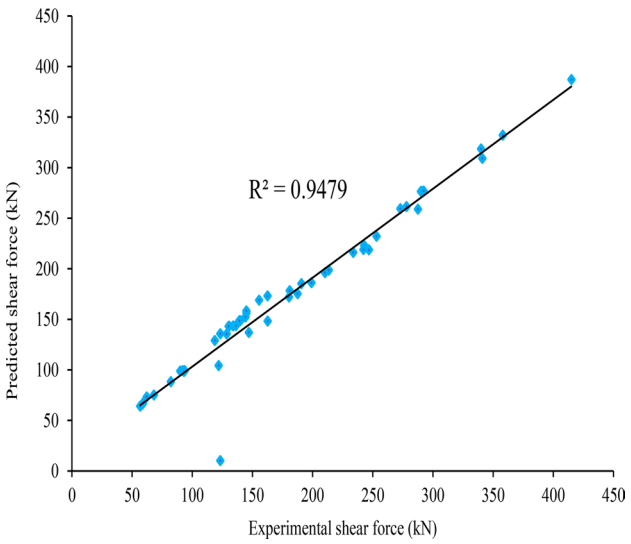

Fig. 6 Predicted and experimental shear forces for the proposed EML model

as d varies from 9.5mm to 30mm, $f_c^{'}$ ranges from 18.3MPa to 109.3MPa, f_u varies from 305.7MPa to 595MPa, and P_u varies from 26.2kN to 415kN. For model development, a normalization of the data is performed using these parameters before presenting the input patterns to statistical machine learning algorithms. Thus, Eq. (10) has been used for the linear normalization of the data values between 0 and 1.

$$x_i^n = \frac{x_i^a - x_i^{min}}{x_i^{max} - x_i^{min}} \tag{10}$$

where, x_i^a and x_i^n are the i^{th} components of the input vector before and after normalization, respectively. x_i^{max} and x_i^{min} are the maximum and minimum values of all components of the input vector before normalization. A typical flowchart for the development of the models is presented in Fig. 4. After developing the models, the normalized output vector obtained from the model is to convert back to the original value by using the following equation.

$$x_i^a = x_i^n\left(x_i^{max} - x_i^{min}\right) + x_i^{min} \tag{11}$$

where, x_i^n is the normalized result obtained after the test for the i^{th} component and x_i^a is the actual result obtained for the i^{th} component, respectively. The efficiency of MPMR and EML models is also related to the assumed design values of ε and σ. In this work, the final values of ε and σ are 0.04 and 0.2 for the MPMR model and 0.03 and 0.3 for the case of EML model. Figures 5 and 6 show the predicted vs experimental shear forces for MPMR and EML, respectively. From Figs. 5 and 6, it can be clearly seen that the models predicted the shear capacity very closely with the experimental values. In addition, the maximum percentage difference between the predicted and the corresponding experimental values are in the range of 10 to 15. Hence, the models developed based on the concept of EML and MPMR are found to be the most reliable and robust.

The capability of MPMR and EML-based models has been assessed through various statistical parameters used for measuring the model's predictive accuracy; namely, (i) root mean square error (RMSE), (ii) mean absolute error (MAE), (iii) coefficient of efficiency (E), (iv) root mean square error to observation's standard deviation ratio (RSR), (v) normalized mean bias error (NMBE), (vi) performance index (ρ), and (vii) variance account factor (VAF). The corresponding equations of these parameters are given below:

$$RMSE = \sqrt{\frac{\sum_{i=1}^{n}\left(C_{cai} - C_{cpi}\right)^2}{N}} \tag{12}$$

$$MAE = \frac{\sum_{i=1}^{n}\left|C_{cai} - C_{cpi}\right|}{N} \tag{13}$$

$$E = 1 - \frac{\sum_{i=1}^{N}\left(C_{cai} - C_{cpi}\right)^2}{\sum_{i=1}^{N}\left(C_{cai} - \overline{C}_{ca}\right)} \tag{14}$$

$$RSR = \frac{RMSE}{\sqrt{\frac{1}{N}\sum_{i=1}^{N}\left(C_{cai} - \overline{C}_{ca}\right)}} \tag{15}$$

$$NMBE(\%) = \frac{1/N\sum_{i=1}^{N}\left(C_{cpi} - C_{cai}\right)}{N\sum_{i=1}^{N}C_{cai}} \tag{16}$$

$$\rho = \frac{RMSE}{\overline{C}_{ca}} \times \frac{1}{R+1} \tag{17}$$

$$VAF = \left(1 - \left(\frac{\mathrm{var}\left(C_{ca} - C_{cp}\right)}{\mathrm{var}\left(C_{ca}\right)}\right)\right) \times 100 \tag{18}$$

where, C_{ca} is the actual shear force, C_{cp} is the predicted shear force, $\overline{C}_{ca}$ is the mean shear force, and var is variance, and N is the number of datasets.

A good model should have (i) the E value near one, (ii) the value of RSR and ρ be small, (iii) a lower positive value or negative value of $NMBE$, indicating over prediction or under prediction, respectively, (iv) the VAF near to 100, and (v) the value of $RMSE$ and MAE should be small. Table 3 lists all the statistical parameters obtained for MPMR and EML models.

Based on the results in Table 3, it can be obtained that (i) $RMSE$, MAE, RSR, and ρ are low, (ii) the value of E is close to one, and (iii) VAF is close to 100. Hence, all the evaluated statistical parameters show that the developed models are efficient and reliable. As given in Fig. 5 for MPMR and Fig. 6 for EML, both models are in very close agreement with experimental results and can be employed for

Table 3 Statistical parameters of the developed MPMR and EML models

Parameters	MPMR		EML	
	Training	Testing	Training	Testing
RMSE	0.031	0.073	0.038	0.088
MAE	0.015	0.032	0.017	0.036
E	0.986	0.948	0.972	0.954
RSR	0.554	1.366	0.682	1.476
NMBE (%)	2.233	5.021	1.996	4.643
ρ	0.852	1.208	1.361	0.991
VAF	91.92	89.01	97.12	93.01

the prediction of the shear strength of headed steel studs in steel–concrete composite structures.

The efficiency of the developed models was also evaluated using well-known engineering indices. The coefficient of determination R-squared (R^2) is a statistical measure of how close the data is to the fitted regression line with values between 0 and 100%. 0% means that the model explains no variability in the response data around its mean, while 100% means that the model explains variability in the response data around its mean. The higher R^2, the better model fits the data. In the present investigation, the MPMR-based model with R^2 of 0.9913, and the EML-based model with R^2 of 0.9479 is a higher performance capacity for prediction, respectively, indicating that the fitted regression of the predicted value is closer to the experimental data. Therefore, it can be said that there is an improved forecasting accuracy with MPMR and EML while making the running time substantially faster, regarding results based on the findings for the investigated scope in the present research.

6 Comparison of MPMR and EML-Based Models with Existing Calculation Methods

In the previous investigations, few models were developed to describe some of the techniques for predicting the shear capacity of headed steel studs in steel–concrete composite structures. In Abambres and He (2019), for example, ANN modeling concepts are applied to determine the shear capacity of headed steel studs. They proposed ANN-based model soft computing expressions regarding applicability and capability and demonstrated that ANN-based models performed better than code-based equations (e.g., given by EC4 2004, AASHTO-LRFD 2014, and GB50017 2017). The equations from EC4, AASHTO-LRFD, and GB50017 are referenced below.

The input parameters for the MPMR and ELM used here to obtain robust models were also used to create the ANN-based model in Abambres and He (2019). To illustrate this, this paper briefly compared the analytical conclusions from MPMR and EML-based models, developed here, with ANN-based models (Abambres & He, 2019) using the same compelling and clear data. According to Abambres and He (2019), the minimum and maximum values for the ratio of predicted and corresponding experimental shear strength capacity (P_u^{ANN}/P_u^E) vary between $0.97 - 1.02$ and hence the average ratio value for the ANN-based model is calculated as 0.99.

On the other hand, variations of the ratio of predicted and corresponding experimental shear strength capacity in the MPMR-based model (P_u^{MPMR}/P_u^E) were in the range of 0.86 to 1.24, and variations of the ELM-based model (P_u^{ELM}/P_u^E) were in between 0.86 and 1.18. Detailed comparisons of the

Table 4 Comparison of experimental values with analytical solutions

$P_u^E(kN)$	$P_u^{MPMR}(kN)$	P_u^{MPMR}/P_u^E	$P_u^{ELM}(kN)$	P_u^{ELM}/P_u^E
122.9	106.3	0.86^{MIN}	148.32	0.91
235.5	216.4	0.92	99.3	1.08
59.4	65.7	1.11	120.3	0.98
93.1	99.65	1.07	65.9	1.13
184.3	172.8	0.94	136.9	0.93
142.1	156.2	1.10	196.2	0.93
253.6	237.1	0.93	276.3	0.95
129.9	136.8	1.05	309.1	0.91
26.2	32.6	1.24^{MAX}	143.5	1.07
381	354.2	0.93	216.2	0.93
174.9	171.3	0.98	172.1	0.95
88.9	98.4	1.11	186.2	0.94
154.4	163.4	1.06	129.1	1.09
135.5	142.6	1.05	143.2	1.10
161	168.2	1.04	173.2	1.07
151.9	157.3	1.04	64.2	1.13
93.8	99.3	1.06	276.5	0.95
60.9	67.9	1.11	135.6	1.05
110.9	116.3	1.05	261.5	0.94
98.8	104.2	1.05	223.1	0.92
331	303.1	0.92	387.1	0.93
138.8	148.1	1.07	332.1	0.93
342	311.7	0.91	75.1	1.10
153.8	164.2	1.07	318.5	0.94
129.3	137.8	1.07	104.3	0.86^{MIN}
70.2	79.2	1.13	98.9	1.10
60.3	67.2	1.11	232.1	0.92
38.5	43.1	1.12	135.8	1.10
147.1	157.2	1.07	219.1	0.90
220.8	204.7	0.93	156.2	1.08
270.2	258.4	0.96	276.9	0.95
214.9	203.6	0.95	158.3	1.09
317	289.5	0.91	67.3	1.14
123	132.1	1.07	198.6	0.93
190.7	182.6	0.96	185.3	0.97
121	128.4	1.06	88.4	1.08
197.2	191.4	0.97	178.4	0.99
92.1	98.5	1.07	99.3	1.06
127.9	135.8	1.06	99.1	1.06
224.3	204.3	0.91	218.8	0.89
176.3	163.2	0.93	259.4	0.95
134.2	145.2	1.08	143.7	1.06
181.6	168.2	0.93	148.6	1.06
224.5	203.1	0.90	152.4	1.06
204	192.1	0.94	258.9	0.90
222	201.3	0.91	143.1	1.10
114.95	122.1	1.06	73.2	1.18^{MAX}
84.4	93.1	1.10	175.4	0.94
189	176.2	0.93	98.4	1.06
56	65.1	1.16	148.6	1.07

Table 4 (continued)

$P_u^E(kN)$	$P_u^{MPMR}(kN)$	P_u^{MPMR}/P_u^E	$P_u^{ELM}(kN)$	P_u^{ELM}/P_u^E
415	387.1	0.93	168.9	1.09
			205.3	0.91

experimental values with the predictions of MPMR and EML are presented in Table 4. As a comparison, the average ratios P_u^{MPMR}/P_u^E and P_u^{ELM}/P_u^E for the MPMR, and EML-based models are calculated as 1.05, and 1.02, respectively. According to the results presented in this paper, a satisfactory performance target, such as a reduced convergence on the scattering amplitudes of numerical results to experimental ones, was achieved using the newly developed MPMR and EML-based models. Although calculation methods are powerful soft computing techniques and offer similar results, MPMR and EML-based models run considerably faster, based on the accuracy for the scope of this study. MPMR and EML-based models perform significantly better than ANN-based model at estimating the shear capacity of headed steel studs due to their beneficial capability. That is, MPMR and EML are said to lead to improved forecasting accuracy more quickly.

EC4 (2004) determines the stud shear strength ($P_{u\_code}^{EC4}$) by the following formula:

$$P_{u\_code}^{EC4} = 0.29\alpha d^2\sqrt{E_c f_c'}/\gamma_v \le 0.8A_s f_u/\gamma_v \tag{19}$$

where, d is the diameter of the stud shank, E_c is the Young's modulus of concrete, $\gamma_v = 1.25$ is the material safety factor, and $A_s = \pi d^2/4$ is the cross-sectional area of a headed stud, respectively. The aspect ratio factor, α, is determined by

$$\alpha = 0.2\left(h_s/d + 1\right), if\ 3 \le h_s/d \le 4 \tag{20}$$

$$\alpha = 1.0, if\ h_s/d > 4 \tag{21}$$

where, h_s refers to the length of the headed stud.

As stated in AASHTO-LRFD (2014), the shear strength ($P_{u\_code}^{AASHTO-LRFD}$) of one stud shear connector embedded in the RC deck is as follows:

$$P_{u\_code}^{AASHTO-LRFD} = 0.5A_s\sqrt{E_c f_c'} \le \phi_{sc}A_s f_u \tag{22}$$

where, $\phi_{sc} = 0.85$ represents the resistance safety factor.

GB50017 (2017) provides the following formula for calculating the design shear strength of a headed steel stud ($P_{u\_code}^{GB50017}$):

$$P_{u\_code}^{GB50017} = 0.43A_s\sqrt{E_c f_c} \le 0.7\gamma A_s f_u \tag{23}$$

where, f_c is the compressive strength of cubic concrete and $\gamma \ge 1.25$ is the ratio of the minimum tensile strength to the yield stress of the headed steel stud.

In regard to EC4 (2004), AASHTO-LRFD (2014), and GB50017 (2017), using this data, the average ratios; $P_{u\_code}^{EC4}/P_u^E$, $P_{u\_code}^{AASTHO-LRFD}/P_u^E$, $P_{u\_code}^{GB50017}/P_u^E$ were calculated as 0.63, 0.84 and 0.87, respectively (Abambres & He, 2019). As compared with experimental values, the codes (AASHTO, 2014; EC4, 2004; GB, 2017) of practice seem to underestimate the shear capacity. Geometric and material properties of specimens affect predictions of three codes (AASHTO, 2014; EC4, 2004; GB, 2017) with different percentages. Specification-defined calculation methods are used within specific limits. Therefore, the specifications showed that these design models underestimated the shear capacity of headed steel studs in steel–concrete composite structures.

7 Conclusions

It is common to employ headed studs as shear connectors in the steel–concrete composite system to derive the maximum benefit of steel and concrete. The headed steel studs are primarily used in the steel–concrete composite system to transfer the longitudinal shear force at the interface of steel and concrete. In the present paper, two regression models were developed based on the concepts of MPMR and EML to predict the shear resistance of headed studs in a steel–concrete composite system. The experimental data on the shear capacity of headed studs were sourced from the literature. The data based on push-out tests (234) were collected and identified the influencing parameters on the shear strength of the headed stud. The identified parameters include (i) steel stud shank diameter, (ii) the compressive strength of concrete, and (iii) the tensile strength of steel stud as input parameter and the shear force as an output parameter. As the input and output data have different quantitative limits (shank diameter varies from 9.5mm to 30mm, the compressive strength of concrete varies from 18.3MPa to 109.3MPa, tensile strength varies from 305.7MPa to 595MPa, and shear force varies from 26.2kN to 415kN), the data have been normalized between 0 and 1 before inputting to the model. From the total dataset, about 70–75% of the mixed dataset comprising the range of values was utilized for developing MPMR and EML based models. The remaining dataset was utilized for the validation of the developed models. The models were developed within MATLAB® environment. As the performance of the MPMR and EML models is primarily dependent on the value of ε and σ, the values of the same have been fixed after several trials. The final values are 0.04 and 0.2 for the MPMR model, and 0.03 and 0.3 for the EML model, respectively.

- The predicted shear force by using the developed models is in close agreement with the corresponding experimental values. It is observed that the predicted shear strength capacity is comparable with the experimental observations. It is found that the R^2 value is 0.9913 and 0.9479, respectively, for the models developed based on the concepts of MPMR and EML, indicating that the predicted value is closer to the experimental data. The ratio of predicted and the corresponding experimental shear strength capacity in the MPMR-based model (P_u^{MPMR}/P_u^E) was in the range of 0.86 to 1.24 while the variations of the EML-based model (P_u^{ELM}/P_u^E) were in between 0.86 and 1.18. As can be seen, by the fact that the predicted and actual values of the shear capacity agree quite well, this is a robust model.
- The efficacy of developed models has also been verified through various statistical parameters, namely, *RMSE*, *MAE*, *E*, *RSR*, *NMBE*, ρ, and *VAF*. The evaluated statistical parameters indicated that the developed models are robust, reliable, and can be applicable for predicting the shear capacity of studs.
- A comparison is included between the performance of analytical solutions/models (e.g., EC4, AASHTO-LRFD, GB50017, ANN) and the MPMR and EML-based models improved in this present study based on the same data. Moreover, the existing design specifications for steel heads in steel-composite structures were reviewed to validate the input data considered, which affects the shear capacity.

To conclude, both MPMR and EML-based models are novel solutions and useful and remarkable contributions for the existing knowledge base and engineers for the prediction of shear capacity of headed steel studs and in turn for the design of steel–concrete composite structures.

Funding No funding was received to assist with the preparation of this paper.

Data Availability Some or all data, models, or code generated or used during the study are available from the corresponding author by request.

Declarations

Conflict of interest The author has no conflicts of interest to declare that are relevant to the content of this article.

References

Abambres, M., & He, J. (2019). Shear capacity of headed studs in steel-concrete structures: analytical prediction via soft computing. Publication No. hal-02074833v3. https://doi.org/10.2139/ssrn.3368670

Akbas, B., Shen, J., & Sabol, T. A. (2011). Estimation of seismic-induced demands on column splices with a neural network model. *Applied Soft Computing, 11*(8), 4820–4829. https://doi.org/10.1016/j.asoc.2011.06.019

Al-Musawi, A. A. (2019). Determination of shear strength of steel fiber RC beams: Application of data-intelligence models. *Frontiers of Structural and Civil Engineering, 13*, 667–673. https://doi.org/10.1007/s11709-018-0504-4

American Association of State Highway and Transportation Officials (AASHTO) (2014). *AASHTO-LRFD Bridge Design Specifications*. AASHTO.

ANSI/AISC-360-16. (2016). American Institute for Steel Construction (AISC). Specification for structural steel buildings, ANSI/AISC 360-16. American Institute for steel Construction. https://www.aisc.org/globalassets/aisc/publications/standards/a360-16-spec-and-commentary_march-2021.pdf

ANSI/AISC 341-16. (2016). Seismic provisions for structural steel buildings. American Institute of Steel Construction. https://www.aisc.org/globalassets/aisc/publications/standards/seismic-provisions-for-structural-steel-buildings-ansi-aisc-341-16.pdf

Avci-Karatas, C. (2019). Prediction of ultimate load capacity of concrete-filled steel tube columns using multivariate adaptive regression splines (MARS). *Steel & Composite Structures,* 33(4), 583–594. https://doi.org/10.12989/scs.2019.33.4.583

Avci-Karatas, C. (2021). Modeling approach for estimation of ultimate load capacity of concrete-filled steel tube composite stub columns based on relevance vector machine. *Nigde Omer Halisdemir University Journal of Engineering Sciences*. https://doi.org/10.28948/ngumuh.759297

Badie, S. S., Tadros, M. K., Kakish, H. F., Splittgerber, D. L., & Baishya, M. C. (2002). Large shear studs for composite action in steel bridge girders. *Journal of Bridge Engineering, 7*(3), 195–203. https://doi.org/10.1061/(ASCE)1084-0702(2002)7:3(195)

Baran, E., & Topkaya, C. (2012). An experimental study on channel type shear connectors. *Journal of Constructional Steel Research, 74*, 108–117. https://doi.org/10.1016/j.jcsr.2012.02.015

Cao, Y., Wakil, K., Alyousef, R., Jermsittiparsert, K., Ho, L., Alabduljabbar, H., Alaskar, A., Alrshoudi, F., & Mohamed, A. M. (2020). Application of extreme learning machine in behavior of beam to column connections. *Structures, 25*, 861–867. https://doi.org/10.1016/j.istruc.2020.03.058

Chen, J., Wang, W., Ding, F. X., Xiang, P., Yu, Y. J., Liu, X. M., Xu, F., Yang, C. Q., & Long, S. G. (2019). Behavior of an advanced bolted shear connector in prefabricated steel-concrete composite beams. *Materials (basel), 12*(18), 2958. https://doi.org/10.3390/ma12182958

Colajanni, P., Mendola, L. L., & Monaco, A. (2014). Stress transfer mechanism investigation in hybrid steel trussed–concrete beams by push-out tests. *Journal of Constructional Steel Research, 95*, 56–70. https://doi.org/10.1016/j.jcsr.2013.11.025

Dennis, L. (2007). Capacities of headed stud shear connectors in composite steel beams with precast hollowcore slabs. *Journal of Constructional Steel Research, 63*, 1160–1174. https://doi.org/10.1016/j.jcsr.2006.11.012

DeRousseau, M. A., Laftchiev, E., Kasprzyk, J. R., Rajagopalan, B., & Srubar, W. V. (2019). A comparison of machine learning methods for predicting the compressive strength of field-placed concrete. *Construction and Building Materials, 228*, 116661. https://doi.org/10.1016/j.conbuildmat.2019.08.042

Dogan, O., & Roberts, T. M. (2012). Fatigue performance and stiffness variation of stud connectors in steel-concrete-steel sandwich systems. *Journal of Constructional Steel Research, 70*, 86–92. https://doi.org/10.1016/j.jcsr.2011.08.013

Driscoll, G.C., & Slutter, R.G. (1961). Research on composite design at Lehigh University, In: Proceedings of the thirteenth national engineering conference of AISC, Reprint No. 180 (61–8), Fritz Laboratory Reports. 279.9, Minneapolis, USA. http://preserve.lehigh.edu/engr-civil-environmental-fritz-lab-reports/1814

Dutta, S., Samui, P., Kim, D. Comparison of machine learning techniques to predict compressive strength of concrete. *Computers and Concrete,* 21(4), 463–470 (2018). https://doi.org/10.12989/cac.2018.21.4.463

Ellobody, E. (2014). Nonlinear material behavior of the Bridge components. *Finite element analysis and design of steel and steel-concrete composite bridges* (1st ed., Chapter 2–3, pp. 47–111). https://doi.org/10.1016/B978-0-12-417247-0.00002-8

Ellobody, E., & Young, B. (2006). Performance of shear connection in composite beams with profiled steel sheeting. *Journal of Constructional Steel Research, 62*(7), 682–694. https://doi.org/10.1016/j.jcsr.2005.11.004

Eurocode 4 (EC4): EN 1994-1-1. (2004) (English) *Design of composite steel and concrete structure –Part 1–1: General rules and rules for buildings (pp. 117)*. CEN, Brussels: European Committee for Standardization. Authority: The European Union per Regulation 305/2011, Directive 98/34/EC, Directive 2004/18/EC]. https://eurocodes.jrc.ec.europa.eu/showpage.php?id=134

Gattesco, N., & Giuriani, E. (1996). Experimental study on stud shear connectors subjected to cyclic loading. *Journal of Constructional Steel Research, 38*(1), 1–21. https://doi.org/10.1016/0143-974X(96)00007-7

GB 50017-2017. (2017). *Code for design of steel structures (English Version Chinese Standard). National Standard of the People's Republic of China (P26)*, 2017-12-12. https://www.chinesestandard.net/PDF.aspx/GB50017-2017

Gholampour, A., Mansouri, I., Kisi, O., & Ozbakkaloglu, T. (2020). Evaluation of mechanical properties of concretes containing coarse recycled concrete aggregates using multivariate adaptive regression splines (MARS), M5 model tree (M5Tree), and least squares support vector regression (LSSVR) models. *Neural Computing and Applications, 32*, 295–308. https://doi.org/10.1007/s00521-018-3630-y

Gopinath, K. G. S., Pal, S., & Tambe, P. (2018). Prediction of hardness and fracture toughness in liquid-phase-sintered alumina system using gaussian process regression and minimax probability machine regression. *Materials Today Proceedings, 5*(5), 12223–12232. https://doi.org/10.1016/j.matpr.2018.02.199

Han, Q. H., Wang, Y. H., Xu, J., Xing, Y., & Yang, G. (2017). Numerical analysis on shear stud in push-out test with crumb rubber concrete. *Journal of Constructional Steel Research, 130*, 148–158. https://doi.org/10.1016/j.jcsr.2016.12.008

Hawkins, N.M. (1973). The strength of stud shear connectors. Institution of Engineers (Australia). *Civil Engineering Translation*, CE15(1), 46–52.

He, J., Liu, Y., Chen, A., & Yoda, T. (2010). Experimental study on inelastic mechanical behaviour of composite girders under hogging moment. *Journal of Constructional Steel Research, 66*(1), 37–52. https://doi.org/10.1016/j.jcsr.2009.07.005

Hiragi, H., Matsui, S., Sato, T., Al-Sakkaf, A., Ishizaki, S., & Ishihara, Y. (2003). Pull-out and shear strength equations for headed studs considering edge distance. *Structural Engineering/earthquake Engineering, 20*(1), 69–80.

Huang, C., & Huang, S. (2020). Predicting capacity model and seismic fragility estimation for RC bridge based on artificial neural network. *Structures, 27*, 1930–1939. https://doi.org/10.1016/j.istruc.2020.07.063

Huang, G. B., & Babri, H. A. (1998). Upper bounds on the number of hidden neurons in feedforward networks with arbitrary bounded nonlinear activation functions. *IEEE Transactions on Neural Networks, 9*(1), 224–229. https://doi.org/10.1109/72.655045

Huang, G. B., Zhu, Q. Y., & Siew, C. K. (2006a). Real-time learning capability of neural networks. *IEEE Transactions on Neural Networks, 17*(4), 863–878. https://doi.org/10.1109/TNN.2006.875974

Huang, G. B., Zhu, Q. Y., & Siew, C. K. (2006b). Extreme learning machine: Theory and applications. *Neurocomputing, 70*(1), 489–501. https://doi.org/10.1016/j.neucom.2005.12.126

Kim, J. S., Kwark, J., Joh, C., Yoo, S. W., & Lee, K. C. (2015). Headed stud shear connector for thin ultrahigh-performance concrete bridge deck. *Journal of Constructional Steel Research, 108*, 23–30. https://doi.org/10.1016/j.jcsr.2015.02.001

Lam, D., & El-Lobody, E. (2005). Behavior of headed stud shear connectors in composite beam. *Journal of the Structural Engineering. American Society of Civil Engineers, 131*(1), 96–107. https://doi.org/10.1061/(ASCE)0733-9445(2005)131:1(96)

Lanckriet, G. R. G., Ghaoui, L. E., Bhattacharyya, C., & Jordan, M. I. (2002). Minimax probability machine. In: T. G. Dietterich, S. Becker, & Z. Ghahramani (Eds.), *Proceedings of the 2001 neural information processing systems (NIPS) conference*. MIT Press

Lin, Z., Liu, Y., & He, J. (2014). Behavior of stud connectors under combined shear and tension loads. *Engineering Structures, 81*, 362–376. https://doi.org/10.1016/j.engstruct.2014.10.016

Mansouri, I., Kisi, O., Sadeghian, P., Lee, C. H., & Hu, J. W. (2017). Prediction of ultimate strain and strength of FRP-confined concrete cylinders using soft computing methods. *Applied Sciences, 7*(8), 751. https://doi.org/10.3390/app7080751

Mansouri, I., Shariati, M., Safa, M., Ibrahim, Z., Tahir, M. M., & Petkovic, D. (2019). Analysis of influential factors for predicting the shear strength of a V-shaped angle shear connector in composite beams using an adaptive neuro-fuzzy technique. *Journal of Intelligent Manufacturing, 30*, 1247–1257. https://doi.org/10.1007/s10845-017-1306-6

Menzies, J. B. (1971). CP 117 and shear connectors in steel-concrete composite beams made with normal-density or lightweight concrete. *Institution of Structural Engineers, 49*(3), 137–154.

Murthy, A.R., Vishnuvardhan, S., Saravanan, M., Gandhi, P. Relevance vector based approach for the prediction of stress intensity factor for the pipe with circumferential crack under cyclic loading. *Structural Engineering and Mechanics,* 72(1), 31–41 (2019). https://doi.org/10.12989/sem.2019.72.1.031

Nguyen, H. T., & Kim, S. E. (2009). Finite element modeling of push-out tests for large stud shear connectors. *Journal of Constructional Steel Research, 65*, 1909–1920. https://doi.org/10.1016/j.jcsr.2009.06.010

Oehlers, D. J., & Johnson, R. P. (1987). The strength of stud shear connections in composite beams. *The Institution of Structural Engineers, 65B*(2), 44–48.

Ollgaard, J., Slutter, R.G., & Fisher, J.W. (1971). Shear strength of stud connectors in lightweight and normal weight concrete. AISC Eng'g Jr April 1971 (71–10)". Fritz Laboratory Reports; 2010, (1971) http://preserve.lehigh.edu/engr-civil-environmental-fritz-lab-reports/2010. *(AISC) American Institute of Steel Construction Engineering Journal,* 8(2), 55–64

Pallarés, L., & Hajjar, J. F. (2010). Headed steel stud anchors in composite structures, Part I: Shear. *Journal of Constructional Steel Research, 66*(2), 198–212. https://doi.org/10.1016/j.jcsr.2009.08.009

Parab, S., Srivastava, S., Samui, P., & Murthy, A. R. (2014). Prediction of fracture parameters of high strength and ultra high strength concrete beams using gaussian process regression and least squares support vector machine. *CMES - Computer Modeling in Engineering, 101*(2), 139–158. https://doi.org/10.3970/cmes.2014.101.139

Shah, V. S., Shah, H. R., Samui, P., & Murthy, A. R. (2014). Prediction of fracture parameters of high strength and ultra-high strength concrete beams using minimax probability machine regression and extreme learning machine. *Computers, Materials and Continua, 44*(2), 73–84. https://doi.org/10.3970/cmc.2014.044.073

Shanmugam, N. E., & Lakshmi, B. (2001). State of the art report on steel–concrete composite columns. *Journal of Constructional Steel Research, 57*(10), 1041–1080. https://doi.org/10.1016/S0143-974X(01)00021-9

Shariati, M., Mafipour, M. S., Mehrabi, P., Bahadori, A., Zandi, Y., Salih, M. N. A., Nguyen, H., Dou, J., Song, X., & Poi-Ngian, S. (2019). Application of a hybrid artificial neural network-particle swarm optimization (ANN-PSO) model in behavior prediction of channel shear connectors embedded in normal and high-strength concrete. *Applied Sciences, 9*, 5534. https://doi.org/10.3390/app9245534

Shim, C. S., Lee, P. G., & Yoon, T. Y. (2004). Static behavior of large stud shear connectors. *Engineering Structures, 26*(12), 1853–1860. https://doi.org/10.1016/j.engstruct.2004.07.011

Slutter, R.G., & Driscoll, G.C. (1965) Flexural strength of steel and concrete composite beams. [Fritz Laboratory Reports. Paper 1806]. *Journal of the Structural Division (ASCE)*, 91(2), 71–99

Strohmann, T., & Grudic, G. Z. A. (2003). Formulation for minimax probability machine regression. In: S. Thrun, S. Becker, & K. Obermayer (Eds.), *Part of: Advances in neural information processing systems 15 (NIPS 2002)*. MIT Press, pp. 769–776.

Sun, J. (2009). Modelling of chaotic time series using minimax probability machine regression, In: *International conference on communications and mobile computing*. Yunnan, China. https://doi.org/10.1109/CMC.2009.35

Thurlimann, B. Fatigue and static strength of stud shear connectors. *American Concrete Institute (ACI)*, 55(6), 1287–1302 (1959). https://doi.org/10.14359/11421

Valente, I. B., & Cruz, P. J. S. (2009). Experimental analysis of shear connection between steel and lightweight concrete. *Journal of Constructional Steel Research, 65*(10–11), 1954–1963. https://doi.org/10.1016/j.jcsr.2009.06.001

Viest, I.M. Investigation of stud shear connectors for composite concrete and steel T-beams. *ACI Journal Proceedings,* 52(4), 875–892 (1956). https://doi.org/10.14359/11655

Wang, D., & Huang, G. B. (2005) Protein sequence classification using extreme learning machine. In: Proceedings of the 2005 IEEE International Joint Conference on Neural Networks, Montreal, QC, Canada, 3, 1406–1411. https://doi.org/10.1109/IJCNN.2005.1556080

Wang, Q. (2013). Experimental research on mechanical behavior and design method of stud connectors. Doctoral dissertation, Tongji University, Shanghai, China.

Xu, C., Sugiura, K., Masuya, H., Hashimoto, K., & Fukada, S. (2015). Experimental study on the biaxial loading effect on group stud shear connectors of steel-concrete composite bridges. *Journal of Bridge Engineering, 20*(10), 1–14. https://doi.org/10.1061/(ASCE)BE.1943-5592.0000718

Xue, D., Liu, Y., Yu, Z., & He, J. (2012). Static behavior of multi-stud shear connectors for steel-concrete composite bridge. *Journal of Constructional Steel Research, 74*, 1–7. https://doi.org/10.1016/j.jcsr.2011.09.017

Xue, W., Ding, M., Wang, H., & Luo, Z. (2008). Static behavior and theoretical model of stud shear connectors. *Journal of Bridge Engineering, 13*(6), 623–634. https://doi.org/10.1061/(ASCE)1084-0702(2008)13:6(623)

Yang, L., Wang, L., Sun, Y., & Zhang, R. (2010). Simultaneous feature selection and classification via minimax probability machine. *International Journal of Computational Intelligence Systems, 3*(6), 754–760. https://doi.org/10.1080/18756891.2010.9727738

Zhou, A., Dai, H., Liu, Q.W., & Feng, D. (2008). Experimental study on shear-bearing bearing capacity of stud connectors within tension concrete. *Journal of Highway and Transportation Research and Development (English Edition)*. https://doi.org/10.1061/JHTRCQ.0000225

Zhou, Z., Wang, Z., & Sun, X. (2013). Face recognition based on optimal kernel minimax probability machine. *Journal of Theoretical and Applied Information Technology, 48*(3), 1645–1651.